In Vivo Formation of Electron Paramagnetic Resonance-Detectable Nitric Oxide and of Nitrotyrosine Is Not Impaired during Murine Leishmaniasis

SELMA GIORGIO,[1] EDLAINE LINARES,[2] HARRY ISCHIROPOULOS,[3]
FERNANDO JOSÉ VON ZUBEN,[4] AUREO YAMADA,[5]
AND OHARA AUGUSTO[2]*

Departamento de Parasitologia[1] and Histologia,[5] Instituto de Biologia, and Faculdade de Engenharia Elétrica,[4]
Universidade Estadual de Campinas, Campinas, and Departamento de Bioquimica, Instituto
de Quimica, Universidade de São Paulo, São Paulo,[2] Brazil, and Institute for
Environmental Medicine, University of Pennsylvania School
of Medicine, Philadelphia, Pennsylvania[3]

Recent studies have provided evidence for a dual role of nitric oxide (NO) during murine leishmaniasis. To explore this problem, we monitored the formation of NO and its derived oxidants during the course of *Leishmania amazonensis* infection in tissues of susceptible (BALB/c) and relatively resistant (C57BL/6) mice. NO production was detected directly by low-temperature electron paramagnetic resonance spectra of animal tissues. Both mouse strains presented detectable levels of hemoglobin nitrosyl (HbNO) complexes and of heme nitrosyl and iron-dithiol-dinitrosyl complexes in the blood and footpad lesions, respectively. Estimation of the nitrosyl complex levels demonstrated that most of the NO is synthesized in the footpad lesions. In agreement, immunohistochemical analysis of the lesions demonstrated the presence of nitrotyrosine in proteins of macrophage vacuoles and parasites. Since macrophages lack myeloperoxidase, peroxynitrite is likely to be the nitrating NO metabolite produced during the infection. The levels of HbNO complexes in the blood reflected changes occurring during the infection such as those in parasite burden and lesion size. The maximum levels of HbNO complexes detected in the blood of susceptible mice were higher than those of C57BL/6 mice but occurred at late stages of infection and were accompanied by the presence of bacteria in the cutaneous lesions. The results indicate that the local production of NO is an important mechanism for the elimination of parasites if it occurs before the parasite burden becomes too high. From then on, elevated production of NO and derived oxidants aggravates the inflammatory process with the occurrence of a hypoxic environment that may favor secondary infections.

Leishmaniasis is an endemic parasitosis caused by several species of the genus *Leishmania*, an intramacrophage parasite. The severity of disease produced by the diverse species that infect humans varies widely, ranging from cutaneous or mucosal to visceral or diffuse cutaneous infection. The former is generally caused by *Leishmania amazonensis*, a species transmitted mainly in the Amazon region which is associated with localized, benign, cutaneous lesions (25, 53).

In murine models, BALB/c mice develop uncontrolled cutaneous lesions after *L. amazonensis* inoculation (34). In contrast, relatively resistant strains of mice (A/J and C57BL/6) are able to control cutaneous infection (2, 34). Most of our current understanding of the circumstances that lead to different outcomes of leishmaniasis has come from studies of murine *L. major* infection. The resolution and progression of the disease are modulated by preferential activation/expansion of subsets of either Th1 or Th2 cells. Macrophages activated by numerous T-cell-derived cytokines, gamma interferon being the most potent, are capable of killing the parasite (35, 44). Recently, nitric oxide (NO; the International Union of Pure and Applied Chemistry-recommended names for NO and peroxynitrite are nitrogen monoxide and oxoperoxynitrate [−1], respectively) has been implicated in the leishmanicidal activity of these cells

and, consequently, in the resolution of disease. Gamma interferon-treated murine macrophages exhibit increased killing of *L. major* amastigotes that is attributable to NO production via an L-arginine-dependent pathway (24). In addition, increased nitrite/nitrate urinary levels correlated with reduced infection and treatment of resistant mice with inhibitors of NO synthases (NOS) exacerbated the disease (19, 32). Expression of inducible NOS (iNOS) analyzed by either histochemical staining or mRNA production was correlated with resistance to *L. major* in murine models (47). In agreement, mutant mice lacking iNOS were shown to be susceptible to the parasite (54).

However, a few studies have demonstrated that during the late stages of infection the overall ability of susceptible mice to generate NO is not limited (20, 23, 37). Nabors et al. (37) have reported that the levels of iNOS mRNA are high in chronic, nonhealing lesions of mice infected with *L. major*, despite being relatively low in early infection. We demonstrated that the levels of NO detected as hemoglobin nitrosyl (HbNO) complexes in blood of BALB/c mice infected with *L. amazonensis* increase with disease evolution (23). In agreement, Evans et al. (19) have shown that the urinary levels of nitrite/nitrate excreted by BALB/c mice infected with *L. major* increased at late stages of infection. Additionally, we demonstrated the presence of proteins containing nitrotyrosines in the cutaneous lesions of BALB/c mice infected with *L. amazonensis* (4, 23), which is evidence for the formation of nitrating agents derived from NO such as peroxynitrite (7). This potent oxidant, produced by the fast reaction between NO and

* Corresponding author. Mailing address: Departamento de Bioquimica, Instituto de Quimica, Universidade de São Paulo, CxP 26077, 05599-970, São Paulo, SP, Brazil. Phone: 55-11-8183873. Fax: 55-11-8187986 or 55-11-8185579. E-mail: oaugusto@quim.iq.usp.br.
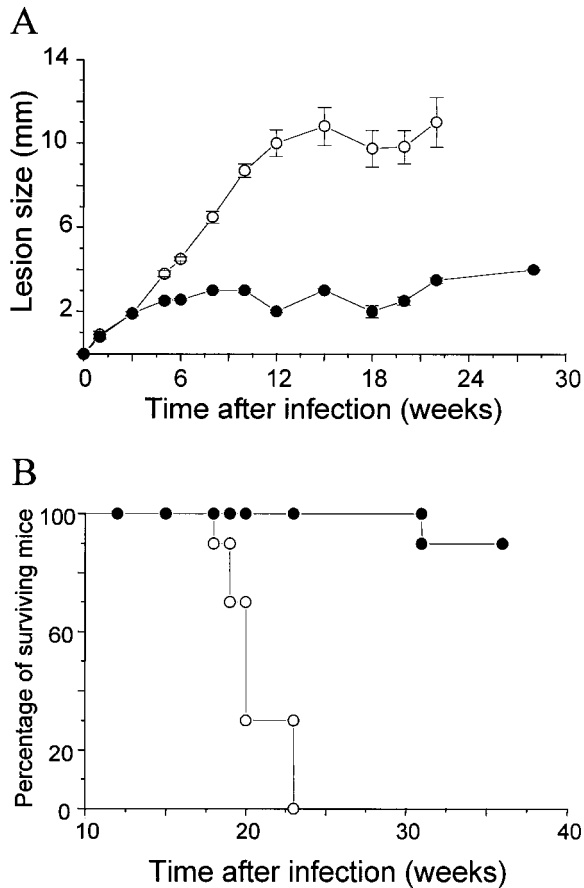
FIG. 1. Course of *L. amazonensis* infection in BALB/c (○) and C57BL/6 (●) mice monitored by lesion size (A) and mortality (B). The animals (10 per group) were injected with 2×10^6 amastigotes. Lesion size is expressed as the difference in size between the infected and contralateral, uninfected footpads. The data shown represent the mean ± standard error of the mean. When not visible, the error bars are smaller than the symbols.

superoxide anion, has been implicated in the pathogenic mechanism of several diseases (3, 7, 8, 29). Since NO and its derived oxidants may play dual roles in either combating or aggravating the disease processes (1, 15, 21, 56), we monitored their formation during the course of *L. amazonensis* infection in tissues of susceptible (BALB/c) and relatively resistant (C57BL/6) mice. Our results demonstrate the formation of NO and derived nitrating agents within macrophages localized in the footpad lesions of both strains, with maximum production occurring at different stages of infection. The late increased NO synthesis detected in the susceptible mice does not eliminate the parasites and appears to contribute to the establishment of secondary infections.

MATERIALS AND METHODS

Parasite and infection. *L. amazonensis* (MHOM/BR/73/M2269) amastigotes were obtained from footpad lesions of BALB/c mice as previously described (5). Female BALB/c and C57BL/6 mice (6 weeks old) were injected subcutaneously in the right hind footpad with 2×10^6 amastigotes.

Evaluation of infection. The course of infection was monitored by measuring the increase in footpad thickness, compared with the contralateral uninfected footpad, with a dial caliper. At designated periods, mice were sacrificed to estimate parasite burdens in the footpad, the popliteal lymph node draining from the site of infection, the spleen, and the liver by a limiting-dilution procedure (51). Data were analyzed with a previously published computer program (50).

Blood and organ collection and EPR measurements. At designated periods, anesthetized mice were bled from the orbital plexus with heparinized pipettes

and tubes. Blood, spleen, footpad tissue, and liver samples perfused with cold phosphate-buffered saline were immediately extruded with a syringe into a quartz tube (2.8- or 4.2-mm inside diameter by 3.8- or 5.0-mm inside diameter, respectively) and frozen in liquid nitrogen. Footpad bone was removed because low-temperature electron paramagnetic resonance (EPR) spectra of the whole footpad minced in liquid nitrogen were dominated by EPR signals of bone components (49). The EPR spectra were obtained with a Bruker ER 200 D-SRC spectrometer by using a fingertip liquid nitrogen dewar. The data were transferred to an IBM/AT computer, where baseline subtraction and double integration were performed. Concentrations of HbNO complexes present in blood and footpad lesions were obtained by double integration of their EPR signal and comparison with the doubly integrated signal from samples of known concentrations prepared by adding saturated solutions of gaseous NO (Alphagaz, São Paulo, Brazil) in phosphate buffer to deoxyhemoglobin solutions (30). The total heme content of blood and footpad samples was determined by the pyridine hemochromogen method after treatment with erythrocyte lysing buffer (Sigma Chemical Co., St. Louis, Mo.). Briefly, after scanning of the EPR spectrum, the footpad tissue (200 to 500 mg) was weighed, treated with lysing buffer (0.50 ml), vortexed, and centrifuged (three times) to obtain a clear supernatant that was diluted with the pyridine hemochromogen reagent; the heme concentration was expressed as nanomoles per gram of tissue.

In some experiments, infected mice were injected intraperitoneally with N^{G}-monomethyl-L-arginine at 50 mg/kg (Sigma Chemical Co.); 3 h later, the animals were bled and heparinized whole blood was immediately introduced into a quartz tube, frozen in liquid nitrogen, and subjected to EPR analysis.

Histopathologic and immunohistochemical analyses. Foot tissues of BALB/c and C57BL/6 mice were obtained after animal perfusion-fixation with 4% paraformaldehyde plus 0.1% glutaraldehyde in 0.1 M phosphate-buffered saline, pH 7.4. Tissues were dehydrated with an ethanol gradient (70 to 100%) and paraffin embedded with Histosec-Merck. Sections were stained with an affinity-purified rabbit polyclonal antinitrityrosine antibody as described previously (28) and counterstained with hematoxylin.

RESULTS

Course of *L. amazonensis* infection in BALB/c and C57BL/6 mice. Mice were injected with 2×10^6 amastigotes, and lesion progression, tissue parasite burden, and survival period were monitored. *L. amazonensis* produced rapidly developing skin
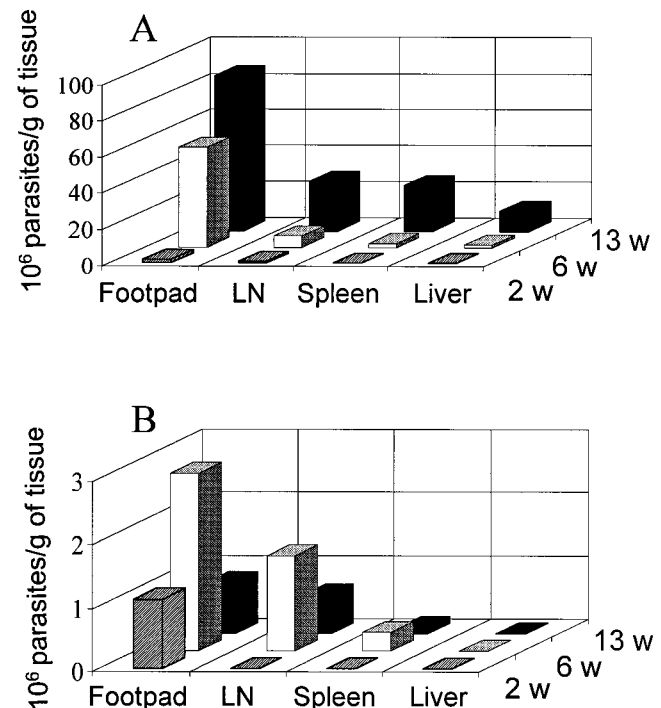

FIG. 2. Tissue parasite burdens in BALB/c (A) and C57BL/6 (B) mice during *L. amazonensis* infection. Animals were infected with 2×10^6 amastigotes. At the indicated weeks (w) after infection, two mice from each group were sacrificed, tissues were collected, and parasite numbers were determined by the limiting-dilution assay. LN, lymph node.
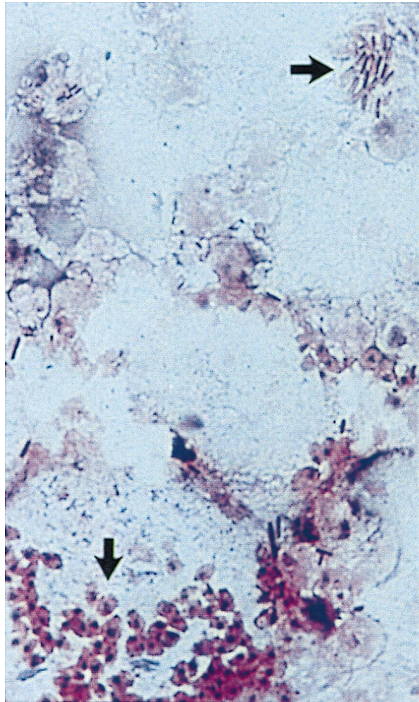
FIG. 3. Representative photomicrograph of a Gram-stained smear prepared from the central necrotic area of a BALB/c mouse lesion at week 22. The bottom and top arrows indicate clusters of *L. amazonensis* amastigotes and bacteria, respectively.
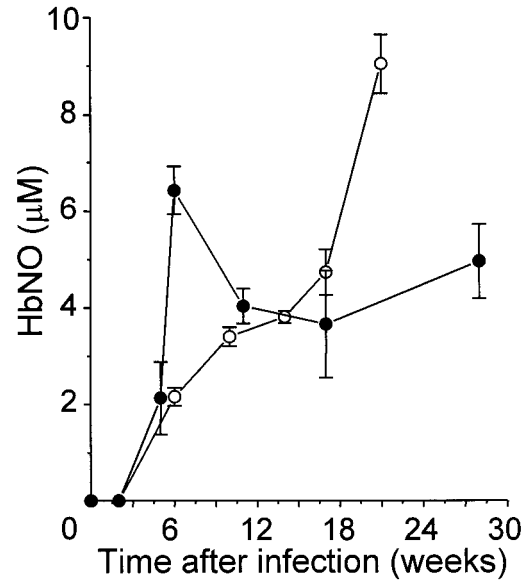

FIG. 4. Levels of HbNO complexes in the blood of BALB/c (○) and C57BL/6 (●) mice during *L. amazonensis* infection. HbNO complex concentrations were determined by low-temperature EPR analysis of the blood of infected animals as described in Materials and Methods. A representative EPR spectrum of the blood drawn from infected mice is shown in Fig. 5A. The data represent the mean ± the standard error of the mean of values obtained from 4 to 10 mice per group at each time point; when not visible, the error bars are smaller than the symbols. HbNO levels in the blood of C57BL/6 mice at week 6 and BALB/c mice at week 22 were significantly ($P \leq 0.05$; Student's *t* test) different from the levels measured in the blood of both strains from weeks 2 to 17.

lesions in BALB/c mice as attested by the continuous increase in footpad thickness (Fig. 1A) up to ulceration, which occurs after about 7 weeks of infection in most animals. No sign of recovery was observed, and after 15 weeks, most mice had developed cutaneous metastatic lesions on the tail and nose. Around week 23, all of the BALB/c mice had died (Fig. 1B). In the C57BL/6 mice, the skin lesions remained controlled, with pad sizes ranging from 4 to 4.5 mm (Fig. 1A). Regression of the disease was not observed up to week 22. In this mouse strain, long-term survival was seen in 90% of the mice (Fig. 1B). Tissue parasite burden analysis indicated that in the C57BL/6 mice, the parasite burden in the footpad, popliteal lymph node, and spleen reached a maximum at week 6 and was decreased by week 13 (Fig. 2B). In contrast, the parasite burden progressively increased with time in all of the examined tissues from BALB/c mice (Fig. 2A). By week 13, the numbers of parasites in the footpad, popliteal lymph node, and spleen were 107-, 45-, and 250-fold higher, respectively, than the numbers found in the same tissues of C57BL/6 mice (Fig. 2A and B).

Interesting to note was the presence of gram-positive rods with spores in Gram-stained smears prepared from the central necrotic area of BALB/c mouse lesions at late stages of infection (17 to 22 weeks) (Fig. 3). These lesions produced the characteristic odor at anaerobic fermentation (38), suggesting secondary infection with *Clostridium* sp.

NO production. The formation of NO during the course of *L. amazonensis* infection was monitored by low-temperature EPR measurements of HbNO complexes in the blood of infected mice (Fig. 4) (23). A representative EPR spectrum of the blood drawn from infected mice is shown in Fig. 5A. This spectrum is qualitatively similar to those previously obtained from blood of other experimental animals producing NO, and it is a composite of two different spectra, one from pentaco-

ordinate HbNO ($g_x \cong 2.07$; $g_z \cong 2.01$; $A_x = A_z \cong 1.7$ mT) and the other from hexacoordinate HbNO ($g_x \cong 2.08$; $g_z \cong 1.98$) (4, 12, 55). The levels of HbNO complexes in blood during *Leishmania* infection reflected enzymatic production of NO because they were strongly reduced by administration of an inhibitor of NOS, N^G-monomethyl-L-arginine, 3 h prior to mouse sacrifice (e.g., Fig. 5).
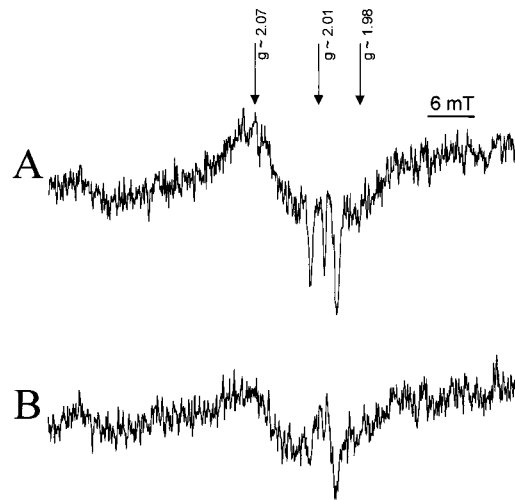

FIG. 5. Representative EPR spectrum of blood drawn from a C57BL/6 mouse after 6 weeks of *L. amazonensis* infection (A). Representative EPR spectrum of blood drawn from a C57BL/6 mouse at the same time of infection, 3 h after treatment with N^G-monomethyl-L-arginine (50 mg/kg) (B). The spectra were run at 77 K. Instrument conditions: microwave power, 10 mW; modulation amplitude, 0.5 mT; time constant, 1 s; scan rate, 0.12 mT/s; gain, 10×10^5.
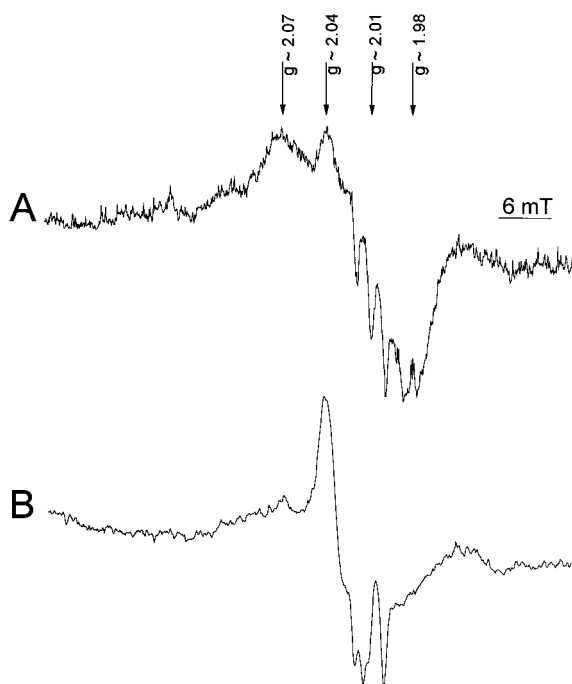
FIG. 6. Representative EPR spectra of footpad lesions of BALB/c (A) and C57BL/6 (B) mice. The footpads were extruded into quartz tubes as described in Materials and Methods. The spectra were run at 77 K. Spectrum A was obtained from one footpad of a BALB/c mouse at week 18 that was extruded into a quartz tube (2.8 by 3.2 mm); spectrum B was obtained from two footpads of two C57BL/6 mice at week 6 that were extruded into a quartz tube (4.2 by 5.0 mm). Instrument conditions: microwave power, 10 mW; modulation amplitude, 0.5 mT; time constant, 1 s; scan rate, 0.12 mT/s; gain, 6.3×10^5 (A) or 4.0×10^5 (B).

In the resistant mice, EPR-detectable levels of HbNO complexes were evident at week 5 and maximum levels (ca. 6.5 μM) were attained at week 6 (Fig. 4), when the parasite load in tissues (footpad, lymph node, and spleen) was at a maximum (Fig. 2B). Thereafter, both the levels of HbNO complexes and the parasite load were reduced but continued production of NO was detectable for up to 28 weeks after infection. In contrast, the levels of HbNO complexes in susceptible BALB/c mice increased marginally (week 6, ca. 2.2 μM; week 14, ca. 3.8 μM) up to the time when metastatic lesions became evident and mortality rates were high (Fig. 1B), and a steep increase in NO production was observed (Fig. 4). Blood from naive C57BL/6 and BALB/c mice (23) did not show EPR-detectable levels of HbNO complexes (data not shown).

Detection of nitrosyl complexes in other tissues of infected mice was also attempted. Target organs of the parasite, such as the liver and spleen, did not present EPR-detectable levels of nitrosyl complexes (data not shown). Livers of both naive and infected mice showed the EPR signals characteristic of normal hepatocytes (12). In contrast, EPR-detectable nitrosyl complexes were detected in the footpad lesions of both strains, and representative spectra are shown in Fig. 6. The marked differences observed in the EPR spectra can be attributed to the diverse tissue architecture of the footpad lesions (Fig. 7) (34). C57BL/6 mouse lesions produced EPR spectra dominated by an axial signal (g $\cong$ 2.04 and g $\cong$ 2.01) characteristic of iron-dithiol-dinitrosyl complexes [Fe(RS)$_2$(NO)$_2$] (Fig. 6B) (6, 17, 31, 57). Detection of the latter species, previously found in activated macrophages and their target cells after induction of NOS (6, 17, 31), demonstrates that nitric oxide is produced in the footpad lesions of infected C57BL/6 mice. The same is true

of infected BALB/c mice, whose footpad lesions produced EPR-detectable heme nitrosyl complexes (Fig. 6A). Some iron-dithiol-dinitrosyl complexes were also present, as evidenced by the peak g $\cong$ 2.04, but the EPR spectra were dominated by signals characteristic of penta- and hexacoordinated heme nitrosyl complexes like those of hemoglobin (Fig. 6A; compare with Fig. 5A). This similarity led us to compare the concentrations of heme nitrosyl complexes present in the lesions of BALB/c mice with those present in the blood of the same animal (Table 1). Parallel determinations of the total heme present in the blood and footpad clearly demonstrated that a much higher percentage of it is bound to NO in the footpad than in the blood (Table 1), indicating that most of the NO is produced in the footpad lesion during *L. amazonensis* infection.

A comparison of the levels of nitrosyl complexes present in the footpads of both strains during the course of infection is more difficult to perform because of the distinct complex signals that predominate in the EPR spectra of each mouse strain (Fig. 6). In addition, the lesions differ markedly in size (Fig. 1) and tissue architecture (Fig. 7). In contrast, blood samples from both mouse strains were comparable and produced the same EPR spectrum (Fig. 5) (4, 23), whose components can be easily quantitated (Fig. 4) (55).

Histopathologic and immunohistochemical analyses for determination of nitrotyrosine in *L. amazonensis*-infected mouse footpads. NO metabolites such as peroxynitrite (3, 7, 8, 27, 29) and nitrite (18, 52) can act as nitrating agents that produce nitrotyrosine residues in proteins. We have previously demonstrated formation of nitrotyrosine in the cutaneous lesions of BALB/c mice at late stages of infection by immunodot blot assay (23). To determine the sites and timing of nitrotyrosine formation, we examined the footpad lesions by immunohistochemical analysis during the course of infection. Examination of footpad lesions of BALB/c and C57BL/6 mice stained for nitrotyrosine residues with hematoxylin counterstain revealed similar profiles at week 2 after *L. amazonensis* infection (Fig. 7A and B). In both mouse strains, the initial lesions showed a mixed cellular population infiltrating the tissue that presents immunoreactivity for nitrotyrosine (Fig. 7A and B).

However, a clear difference was evident in the later stages of infection. At week 6, BALB/c mouse footpad tissue was dominated by parasitized macrophages (Fig. 7C). By week 13, skin lesions continued to demonstrate massive numbers of vacuolated and heavily parasitized macrophages that infiltrated subcutaneous fat and muscle and completely replaced the normal tissue (Fig. 7E). These lesions consistently showed nitrotyrosine staining in the parasitophorous vacuoles of macrophages and in the intracellular amastigotes. In contrast, the lesions of C57BL/6 mice at week 6 were characterized by some parasitized macrophages isolated by a variety of other cell types (Fig. 7D). Later in the infection, these mice were able to decrease their parasite load (Fig. 2B) but a few inflammatory cells could still be observed (Fig. 7F). Immunoreactivity for nitrotyrosine was observed in the inflammatory cells and surrounding tissue (Fig. 7F). Contralateral footpad tissue from BALB/c and C57BL/6 mice showed no immunostaining with the polyclonal antibody for nitrotyrosine (data not shown).

DISCUSSION

The results reported here demonstrated that NO (Fig. 4 to 6) and derived nitrating agents (Fig. 7) are produced during the course of *L. amazonensis* infection (Fig. 1 and 2) in both susceptible and relatively resistant mice. NO production was detected directly by EPR of the produced HbNO complexes in
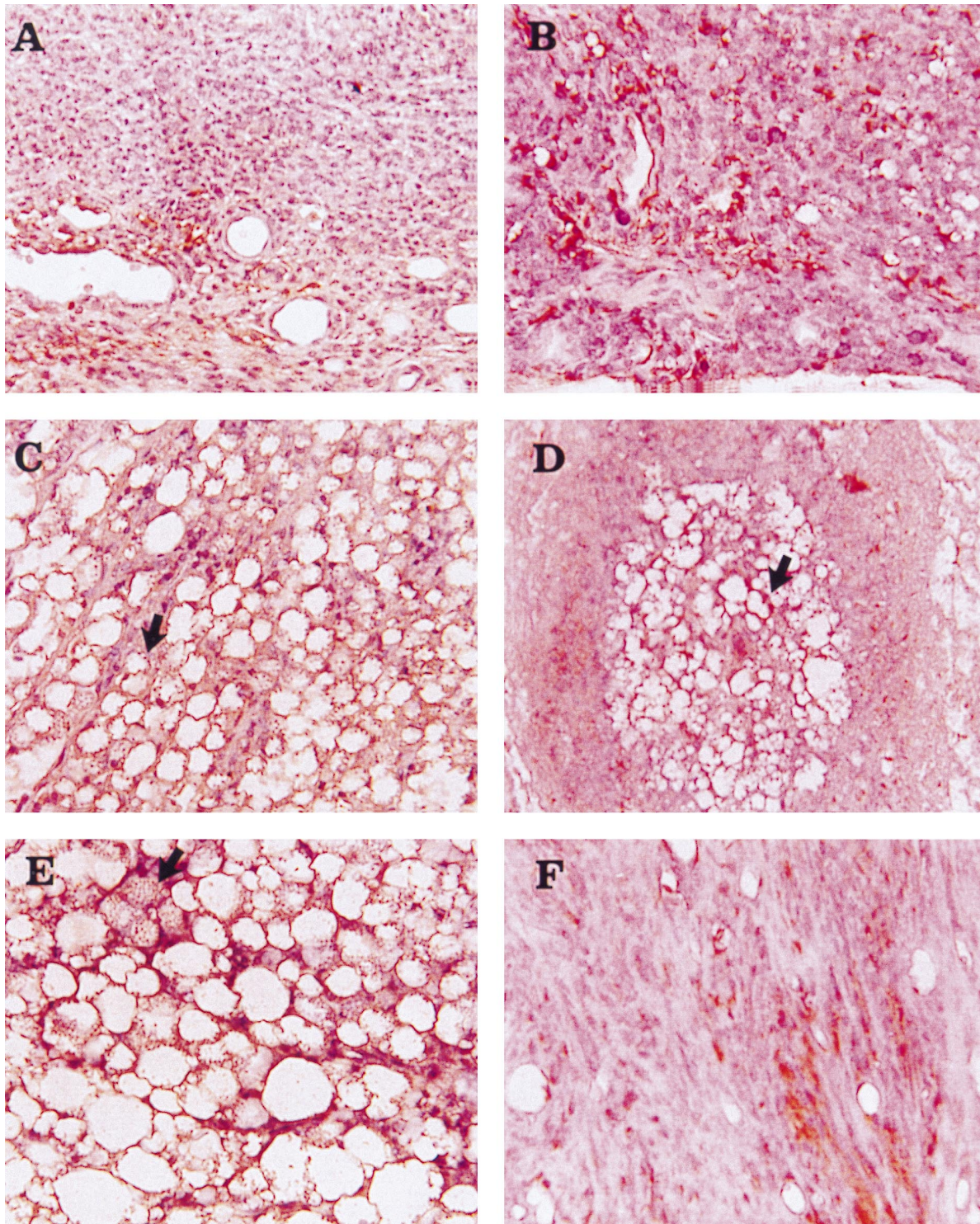
FIG. 7. Photomicrographs of *L. amazonensis*-infected mouse lesion sections. Sections were immunohistochemically stained by using nitrotyrosine polyclonal antibody and counterstained with hematoxylin. The brown reaction product indicates specific binding of the nitrotyrosine antibody. (A) BALB/c footpad lesion at week 2, demonstrating immunoreactivity for nitrotyrosine in the mixed cellular population infiltrating the tissue. (B) C57BL/6 footpad lesion at week 2, demonstrating immunoreactivity for nitrotyrosine in the mixed cellular population infiltrating the tissue. (C) BALB/c footpad lesion at week 6; the arrow indicates a macrophage infected with stained amastigotes. (D) C57BL/6 footpad lesion at week 6; immunostained, infected macrophages are surrounded by a variety of other cell types. (E) BALB/c mouse footpad lesion at week 13; the arrow indicates a vacuolated, infected macrophage with stained intracellular amastigotes. (F) C57BL/6 mouse footpad lesion at week 13; immunoreactivity was observed in the inflammatory cells and the surrounding tissue. The slides were examined with a 25× lens, photographed, and printed under the same conditions.

TABLE 1. Estimation of heme nitrosyl complex levels present in blood and footpads of infected BALB/c mice[a]

Wk after infection	Heme nitrosyl complexes			
	Concn in:		% of total heme[b] in:	
	Blood (μM)	Footpad (nmol/g)	Blood	Footpad
14	3.8	17.0	0.06	14.5
18	4.5	27.6	0.10	26.6

[a] Animal treatment, tissue collection, EPR analysis, and heme analysis were performed as described in Materials and Methods. The values shown are average results obtained with two mice at each time of infection.

[b] The percentage of total heme that appears as heme nitrosyl complexes is shown. Total heme concentrations determined in whole blood and footpad tissues were $6,210 \pm 125$ μM ($n = 18$) and 103.7 ± 18 nmol/g of tissue ($n = 4$), respectively.

whole blood (Fig. 4 and 5) and of heme nitrosyl (Fig. 6A) and iron-dithiol-dinitrosyl complexes (Fig. 6B) in the footpad lesions. Estimation of nitrosyl complex levels in whole blood and footpad lesions (Table 1) demonstrated that most of the NO is synthesized in the cutaneous lesions. This was further proved by the immunohistochemical detection of nitrotyrosine residues in proteins of the parasitophorous vacuoles of macrophages and of their parasites (Fig. 7). Nitrotyrosine residues are produced by attack of protein tyrosines by NO-derived nitrating agents such as peroxynitrite (3, 7, 8, 27, 29) and nitrite (18, 52). Peroxynitrite, produced by the fast reaction between NO and superoxide anion, is a nitrating agent by itself (27), whereas nitrite produces nitrotyrosine upon activation by hypochlorous acid or peroxidase enzymes (18, 52). Macrophages lack myeloperoxidase (45), and consequently, peroxynitrite is likely to be the nitrating agent formed during the course of *L. amazonensis* infection. It has been previously reported that expression of iNOS occurs in the cutaneous lesions of mice during *L. major* infection (47). Now, we demonstrate that the enzyme product, NO, is indeed produced in vivo.

To monitor NO production during the course of infection, we measured the levels of HbNO complexes in blood because they are easier to quantitate (see Results) and should reflect the production of NO in tissue. Hemoglobin is likely to act as a final sink for the NO produced in vivo because of its high affinity for the gas and its high concentration in the blood (in the millimolar range), which are much higher than those found for other cell proteins. In agreement, the levels of HbNO complexes found in blood correlated with the heme nitrosyl complexes found in the lesions (Table 1). Moreover, the levels of HbNO complexes in the blood of susceptible and relatively resistant mice (Fig. 4) reflected changes occurring during the course of the infection, such as those in parasite burden (Fig. 2), lesion size (Fig. 1), lesion constitutive tissues (Fig. 7), and formation of nitrotyrosine (Fig. 7).

The maximum levels of HbNO complexes that can be detected during the infection of susceptible mice are higher than those of the relatively resistant mice but occur at different times of infection (Fig. 4). The early increase in NO synthesis observed in the relatively resistant C57BL/6 mice appears to be important for the control of the infection because the parasite burden in tissues decreased thereafter (Fig. 2B). In parallel, NO production decreased but remained detectable for up to 28 weeks after infection (Fig. 4). This continued NO production should be related to the small amounts of *L. amazonensis* that remain in the tissues of the animals (Fig. 2). Stenger et al. (48) have recently demonstrated that *L. major* parasites persist in small numbers in clinically cured mice and are important for

the lifelong expression of iNOS at the site of the original lesion and in the draining lymph node. It is important to note that the increased NO production by C57BL/6 compared with naive or susceptible mice was detectable by week 5 (Fig. 4), and this result agrees with studies performed with other murine models. Indeed, increased urinary excretion of nitrite/nitrate by resistant compared with susceptible mice infected with *L. major* was detectable at about week 2 (20). Also, differences in lesion size between mutant iNOS $-/-$ and wild-type mice were detectable 5 weeks after infection with *L. major* (54). These results suggest that although local NO synthesis within macrophages (Fig. 6 and 7) should be an important mechanism for the elimination of the parasites (9, 20, 54), still unidentified factors may be produced in the early stages of infection and play a role in its control.

Although being formed in considerable quantities, neither NO nor its in vitro leishmanicidal metabolite peroxynitrite (4, 22) is able to control the infection in susceptible mice (Fig. 1 and 7). This is possibly a consequence of the late production of these derivatives that occurs at a stage when the parasite load is enormous (Fig. 2 and 7), secondary infection is occurring (Fig. 3), and the cytotoxic activities of NO, probably exerted through its derived oxidants (10, 16, 22, 46), are not sufficient to eliminate so many pathogens. The reasons why NO synthesis occurs at late stages of infection in susceptible mice remain unknown. It has been suggested that *Leishmania*-infected macrophages are less responsive to macrophage-activating factors (11, 41, 42). If this is true, the late peak of NO synthesis may reflect the enormous number of macrophages present in the lesions at this time of infection (Fig. 7) that should compensate for the inefficiency of the individual cells in synthesizing NO. These macrophages may be responding to parasite-derived products (42) and also to bacterium-derived toxins (12, 14, 43) due to the ongoing secondary infection. The possibility that the parasite itself produces NO cannot be excluded because *Trypanosoma cruzi*, another trypanosomatid, has been shown to express NOS (40).

In conclusion, our results support the view that local production of NO and its derived oxidants in macrophages is an important mechanism for the elimination of intracellular pathogens (9, 13, 33). They emphasize, however, that control of murine *L. amazonensis* infection should depend on still unidentified factors that act in the early stages of infection. Also, they indicate that NO production is effective before the parasite burden becomes too high. From then on, elevated production of NO and derived oxidants appears to aggravate the inflammatory process, facilitating the occurrence of secondary infections. Inflammation is known to lead to a cycle of oxidant injury by recruiting more activated cells that produce increased levels of oxidants and by inducing several hypoxic-reperfusion injury processes due to intermittent vascular occlusion (15, 26, 36, 39). The predominance of a hypoxic environment may lead to the proliferation of anaerobic bacteria such as those detected in the footpad lesions of BALB/c mice. The final outcome is a general decline in health and increased mortality rates.

REFERENCES

1. **Akaike, T., Y. Noguchi, S. Ijiri, K. Setoguchi, M. Suga, Y. M. Zheng, B. Dietzschold, and H. Maeda.** 1996. Pathogenesis of influenza virus-induced pneumonia: involvement of both nitric oxide oxygen radicals. Proc. Natl. Acad. Sci. USA **93:**2448–2453.

2. **Andrade, Z. A., S. G. Reed, S. B. Roters, and M. Sadigursky.** 1984. Immunopathology of experimental cutaneous leishmaniasis. Am. J. Pathol. **114:**137–148.

3. **Augusto, O., and R. Radi.** 1995. Peroxynitrite reactivity: free radical generation, thiol oxidation, and biological significance, p. 83–116. *In* L. Packer and E. Cadenas (ed.), Biothiols in health and disease. Marcel Dekker, Inc., New York, N.Y.

4. **Augusto, O., E. Linares, and S. Giorgio.** 1996. Possible roles of nitric oxide and peroxynitrite in murine leishmaniasis. Braz. J. Med. Biol. Res. **29:**853–862.

5. **Barbiéri, C. L., S. Giorgio, A. J. C. Merjan, and E. N. Figueiredo.** 1993. Glycosphingolipid antigens of *Leishmania* (*Leishmania*) *amazonensis* amastigotes identified by use of a monoclonal antibody. Infect. Immun. **61:**2131–2137.

6. **Bastian, N. R., C.-Y. Yim, J. B. Hibbs, Jr., and W. E. Samlowski.** 1994. Induction of iron-derived EPR signals in murine cancers by nitric oxide. J. Biol. Chem. **269:**5127–5131.

7. **Beckman, J. S.** 1996. Oxidative damage and tyrosine nitration from peroxynitrite. Chem. Res. Toxicol. **9:**836–844.

8. **Beckman, J. S., T. W. Beckman, J. Chen, P. A. Marshall, and B. A. Freeman.** 1990. Apparent hydroxyl radical production by peroxynitrite: implications for endothelial injury from nitric oxide and superoxide. Proc. Natl. Acad. Sci. USA **87:**1620–1624.

9. **Bogdan, C., A. Gessner, W. Solbach, and M. Röllinghoff.** 1996. Invasion, control and persistence of *Leishmania* parasites. Curr. Opin. Immunol. **8:**517–525.

10. **Brunelli, L., J. P. Crow, and J. S. Beckman.** 1995. The comparative toxicity of nitric oxide and peroxynitrite to *Escherichia coli*. Arch. Biochem. Biophys. **316:**327–334.

11. **Buchmüller-Rouiller, Y., and J. Mauël.** 1987. Impairment of the oxidative metabolism of mouse peritoneal macrophages by intracellular *Leishmania* spp. Infect. Immun. **55:**587–593.

12. **Chamulitrat, W., S. J. Jordan, R. P. Mason, A. L. Litton, J. G. Wilson, E. R. Wood, G. Wolberg, and L. M. Vedia.** 1995. Targets of nitric oxide in a mouse model of liver inflammation by *Corynebacterium parvum*. Arch. Biochem. Biophys. **316:**30–37.

13. **Clark, I. A., and K. A. Rockett.** 1996. Nitric oxide and parasitic disease. Adv. Parasitol. **37:**1–56.

14. **Cunha, F. Q., D. W. Moss, L. M. C. C. Leal, S. Moncada, and F. Y. Liew.** 1993. Induction of macrophage parasiticidal activity by *Staphylococcus aureus* and exotoxins through the nitric oxide synthesis pathway. Immunology **78:**563–567.

15. **Darley-Usmar, V., H. Wiseman, and B. Halliwell.** 1995. Nitric oxide and oxygen radicals: a question of balance. FEBS Lett. **369:**131–135.

16. **Denicola, A., H. Rubbo, D. Rodríguez, and R. Radi.** 1993. Peroxynitrite-mediated cytotoxicity to *Trypanosoma cruzi*. Arch. Biochem. Biophys. **304:**279–286.

17. **Drapier, J. C., C. Pellat, and Y. Henry.** 1991. Generation of EPR-detectable nitrosyl-iron complexes in tumor target cells cocultured with activated macrophages. J. Biol. Chem. **266:**10162–10167.

18. **Eiserich, J. P., C. E. Cross, A. D. Jones, B. Halliwell, and A. Van der Vliet.** 1996. Formation of nitrating and chlorinating species by reaction of nitrite with hypochlorous acid. J. Biol. Chem. **271:**19199–19208.

19. **Evans, T. G., L. Thai, D. L. Granger, and J. B. Hibbs, Jr.** 1993. Effect of in vivo inhibition of nitric oxide production in murine leishmaniasis. J. Immunol. **151:**907–915.

20. **Evans, T. G., S. S. Reed, and J. B. Hibbs, Jr.** 1996. Nitric oxide production in murine leishmaniasis: correlation of progressive infection with increasing systemic synthesis of nitric oxide. Am. J. Trop. Med. Hyg. **54:**486–489.

21. **Evans, T. J., L. D. K. Buttery, A. Carpenter, D. R. Springall, J. M. Polak, and J. Cohen.** 1996. Cytokine-treated human neutrophils contain inducible nitric oxide synthase that produces nitration of ingested bacteria. Proc. Natl. Acad. Sci. USA **93:**9553–9558.

22. **Gatti, R. M., O. Augusto, J. K. Kwee, and S. Giorgio.** 1995. Leishmanicidal activity of peroxynitrite. Redox Rep. **1:**261–265.

23. **Giorgio, S., E. Linares, M. L. Capurro, A. G. Bianchi, and O. Augusto.** 1996. Formation of nitrosyl hemoglobin and nitrotyrosine during murine leishmaniasis. Photochem. Photobiol. **63:**750–754.

24. **Green, S. J., M. S. Meltzer, J. B. Hibbs, Jr., and C. A. Nacy.** 1990. Activated macrophages destroy intracellular *Leishmania major* amastigotes by an L-arginine-dependent killing mechanism. J. Immunol. **144:**278–283.

25. **Grimaldi, G., Jr., R. B. Tesh, and D. MacMahon-Pratt.** 1989. A review of the geographic distribution and epidemiology of leishmaniasis in the New World. Am. J. Trop. Med. Hyg. **41:**687–725.

26. **Ischiropoulos, H., A. B. Al-Mehdi, and A. B. Fisher.** 1995. Reactive species in ischemic rat lung injury: contribution of peroxynitrite. Am. J. Physiol. **269:**L158–L164.

27. **Ischiropoulos, H., L. Zhu, J. Chen, M. Tsai, J. C. Martin, C. D. Smith, and J. S. Beckman.** 1992. Peroxynitrite-mediated tyrosine nitration catalyzed by superoxide dismutase. Arch. Biochem. Biophys. **298:**431–437.

28. **Ischiropoulos, H., M. F. Beers, S. T. Ohnishi, D. Fisher, S. E. Garner, and S. R. Thom.** 1996. Nitric oxide production and perivascular tyrosine nitration in brain after carbon monoxide poisoning in the rat. J. Clin. Invest. **97:**2260–2267.

29. **Kooy, N. W., J. A. Royall, Y. Z. Ye, D. R. Kelly, and J. S. Beckman.** 1995. Evidence for *in vivo* peroxynitrite production in human acute lung injury. Am. J. Respir. Crit. Care Med. **151:**1250–1254.

30. **Kruszyna, H., R. Kruszyna, R. P. Smith, and D. E. Wilcox.** 1987. Red blood cells generate nitric oxide from directly acting nitrogenous vasodilations. Toxicol. Appl. Pharmacol. **91:**429–438.

31. **Lancaster, J. R., and J. B. Hibbs, Jr.** 1990. EPR demonstration of iron-nitrosyl complex formation by cytotoxic activated macrophages. Proc. Natl. Acad. Sci. USA **87:**1223–1227.

32. **Liew, F. Y., S. Millott, C. Parkinson, R. M. J. Palmer, and S. Moncada.** 1990. Macrophage killing of *Leishmania* parasite in vivo is mediated by nitric oxide from L-arginine. J. Immunol. **144:**4794–4797.

33. **MacMicking, J., Q. Xie, and C. Nathan.** 1997. Nitric oxide and macrophage function. Annu. Rev. Immunol. **15:**323–350.

34. **McElrath, M. J., G. Kaplan, A. Nusrat, and Z. A. Cohn.** 1987. Cutaneous leishmaniasis. The defect in T cell influx in BALB/c mice. J. Exp. Med. **165:**546–559.

35. **Milon, G., G. Del Giudice, and J. A. Louis.** 1995. Immunobiology of experimental cutaneous leishmaniasis. Parasitol. Today **11:**244–247.

36. **Mulligan, M. S., J. M. Hevel, M. A. Marletta, and P. A. Ward.** 1991. Tissue injury caused by deposition of immune complexes is L-arginine dependent. Proc. Natl. Acad. Sci. USA **88:**6338–6342.

37. **Nabors, G. S., T. Nolan, W. Croop, J. Li, and J. P. Farrell.** 1995. The influence of the site of parasite inoculation on the development of Th1 and Th2 type immune responses in (BALB/c × C57BL/6) F1 mice infected with *Leishmania major*. Parasite Immunol. **17:**569–579.

38. **Onderdonk, A. B., and S. D. Allen.** 1995. *Clostridium*, p. 574–586. *In* P. R. Murray, E. J. Baron, M. A. Pfaller, F. C. Tenover, and R. H. Yolken (ed.), Manual of clinical microbiology, 6th ed. ASM Press, Washington, D.C.

39. **Oury, T. D., C. A. Piantadosi, and J. D. Crapo.** 1993. Cold-induced brain edema in mice. J. Biol. Chem. **268:**15394–15398.

40. **Paveto, C., C. Pereira, J. Espinosa, A. E. Montagna, M. Farber, M. Esteva, M. M. Flawiá, and H. N. Torres.** 1995. The nitric oxide transduction pathway in *Trypanosoma cruzi*. J. Biol. Chem. **270:**16576–16579.

41. **Proudfoot, L., C. A. O'Donnell, and F. Y. Liew.** 1995. Glycoinositolphospholipids of *Leishmania major* inhibit nitric oxide synthesis and reduce leishmanicidal activity in murine macrophages. Eur. J. Immunol. **25:**745–750.

42. **Proudfoot, L., A. V. Nikolaev, G. Feng, X. Wei, M. A. J. Ferguson, J. S. Brimacombe, and F. Y. Liew.** 1996. Regulation of the expression of nitric oxide synthase and leishmanicidal activity by glycoconjugates of *Leishmania* lipophosphoglycan in murine macrophages. Proc. Natl. Acad. Sci. USA **93:**10984–10989.

43. **Rees, D. D., F. Q. Cunha, J. Assreuy, A. G. Herman, and S. Moncada.** 1995. Sequential induction of nitric oxide synthase by *Corynebacterium parvum* in different organs of the mouse. Br. J. Pharmacol. **114:**689–693.

44. **Reiner, S. L., and R. M. Locksley.** 1995. The regulation of immunity to *Leishmania major*. Annu. Rev. Immunol. **13:**151–177.

45. **Rosen, G. M., S. Pou, C. L. Ramos, M. S. Cohen, and B. E. Britigan.** 1995. Free radicals and phagocytic cells. FASEB J. **9:**200–209.

46. **Rubbo, H., A. Denicola, and R. Radi.** 1994. Peroxynitrite inactivates thiol-containing enzymes of *Trypanosoma cruzi* energetic metabolism and inhibits cell respiration. Arch. Biochem. Biophys. **308:**96–102.

47. **Stenger, S., H. Thüring, M. Röllinghoff, and C. Bogdan.** 1994. Tissue expression of inducible nitric oxide synthase is closely associated with resistance to *Leishmania major*. J. Exp. Med. **180:**783–793.

48. **Stenger, S., N. Donhauser, H. Thüring, M. Röllinghoff, and C. Bogdan.** 1996. Reactivation of latent leishmaniasis by inhibition of inducible nitric oxide synthase. J. Exp. Med. **183:**1501–1514.

49. **Symons, M. C. R.** 1996. Radicals generated by bone cutting and fracture. Free Radical Biol. Med. **20:**831–835.

50. **Taswell, C.** 1981. Limiting dilution assays for determination of immunocompetent cell frequencies. I. Data analysis. J. Immunol. **126:**1614–1619.

51. **Titus, R. G., M. Marchand, T. Boon, and J. A. Louis.** 1985. A limiting dilution assay for quantifying *Leishmania major* in tissues of infected mice. Parasite Immunol. **7:**545–555.

52. **Van der Vliet, A., J. P. Eiserich, B. Halliwell, and C. E. Cross.** 1997. Formation of reactive nitrogen species during peroxidase-catalyzed oxidation of nitrite. J. Biol. Chem. **272:**7617–7625.

53. **Walton, B. C.** 1987. American cutaneous and mucocutaneous leishmaniasis, p. 637–664. *In* W. Peters and R. Killick-Kendrick (ed.), Leishmaniases in biology and medicine, vol. 1. Academic Press, London, England.

54. **Wei, X., I. A. Charles, A. Smith, J. Ure, G. Feng, F. Huang, D. Xu, W. Muller, S. Moncada, and F. Y. Liew.** 1995. Altered immune responses in mice lacking

inducible nitric oxide synthase. Nature (London) **375:**408–411.

55. **Westenberger, U., S. Thanner, H. H. Ruf, K. Gersonde, G. Sutter, and O. Trentz.** 1990. Formation of free radicals and nitric oxide derivative of hemoglobin in rats during shock syndrome. Free Radical Res. Commun. **11:** 167–178.

56. **Wizemann, T. M., C. R. Gardner, J. D. Laskin, S. Quinones, S. K. Durham,**

N. L. Goller, T. Ohnishi, and D. L. Laskin. 1994. Production of nitric oxide and peroxynitrite in the lung during acute endotoxemia. J. Leukocyte Biol. **56:**759–768.

57. **Woolum, J. C., E. Tiezzi, and B. Commoner.** 1968. Electron spin resonance of iron-nitric oxide complexes with amino acids, peptides and proteins. Biochim. Biophys. Acta **160:**311–320.

Editor: R. E. McCallum